Supplementary material

Methods

Measurement of pulse wave velocity Pulse wave velocity was measured between the neck and femoral artery (Vicorder®, SMT Medical GmbH&Co., Wurzburg, Germany) as previously described (1).

Measurement of body composition and intracellular fat Total and regional adipose tissue volumes were measured after imaging data was analysed using the SliceOmatic image analysis program (Tomovision, Montreal, Quebec, Canada). All spectra were analysed in the time domain using the AMARES algorithm included in the MRUI software package (2). IMCL was expressed as a ratio to the muscle creatine signal. IHCL was expressed as a % ratio to liver water content. Single slice multi-echo was performed through the pancreas during a single breath hold of fifteen seconds. Typical parameters were field-of-view 400*300mm, repetition time 150 ms, 10mm slice thickness; twenty echo times starting at 1.15ms with spacing of 1.15ms producing alternate in and out of phase images. Analysis was performed using MATLAB to produce a measurement of pancreatic fat as previously described (3).

Laboratory protocols ApoB from both $VLDL_1$ and $VLDL_2$ fractions were selectively precipitated by an equal volume of isopropanol, and extracted with ethanol: diethyl ether (2:1 v/v). The precipitate from the $VLDL_1$-apoB fraction was applied to SDS polyacrylamide gel electrophoresis to isolate apoB100. The isolated $VLDL_1$ and $VLDL_2$-apoB were acid hydrolysed (6M HCl) at 120^{o}C for 24h, purified by ion- exchange (Resin AG® 50W-X8 Resin, Cation Form) and derivatised with trifluoroacetic acid and trifluoroacetic anhydride (4). Isotopic enrichment was measured by negative chemical ionization gas chromatography mass spectrometry (GCMS) (Agilent 5975 inert XL MSD) monitoring the ions m/z 209 and 210.

The lipid content of $VLDL_1$ and $VLDL_2$ fractions at each time point, was extracted with chloroform:methanol (2:1 v/v), isolated by thin layer chromatography, and hydrolysed in the presence of 3% HCL in methanol (v/v) at 50^{o}C overnight. Glycerol was further purified by ion-exchange chromatography (AG® 50W-X8 Resin, Hydrogen Form and AG1-X8 Resin, Formate Form) and

derivatised to form the triacetate derivative (5). Isotopic enrichment of glycerol was measured by positive chemical ionization GCMS (Agilent 5973 network MSD) monitoring the ions m/z 159 and 164. Plasma glycerol enrichment was determined after deproteinisation of plasma using 3.5% sulphosalicylic acid and purified by ion exchange chromatography before derivatisation (5). To measure plasma α KIC enrichment, plasma was extracted with ethanol and reacted with O-phenylenediamine (2% in 4M HCL) at 90 °C for 1 hour, then extracted with ethyl acetate. The extracted residue was redissolved in acetonitrile and derivatised to form a quinoxalinol-TMS derivative of the keto acid (4). Isotopic enrichment was measured by electron ionization GCMS (Agilent 5973 network MSD) monitoring ions m/z 275 and 276.

Plasma glucose, NEFA, TG, $VLDL_1$ and $VLDL_2$-TG and cholesterol and LDL and HDL cholesterol were measured enzymatically using a Cobas MIRA (Roche, Welwyn Garden City, UK). Insulin was measured by immunoassay (Millipore corporation, Billerica, MA, USA). $VLDL_1$ and $VLDL_2$-apoB were measured by an in-house ELISA. ALT, AST and GGT were measured by an Advia 1800 Chemistry System (Siemens Healthcare Diagnostics).

Kinetic modelling of $VLDL_1$ and $VLDL_2$-TG

$VLDL_1$ and $VLDL_2$, TG FCR (pools/d) were determined using SAAM II software. Plasma glycerol kinetics was described by a sum of three exponentials representing a three compartment model. The incorporation of glycerol into VLDL by the liver is subject to a delay. A five-compartment chain described time delay due to synthesis and secretion of $VLDL_1$ and $VLDL_2$-TG. The model is schematically depicted in Fig. 1.

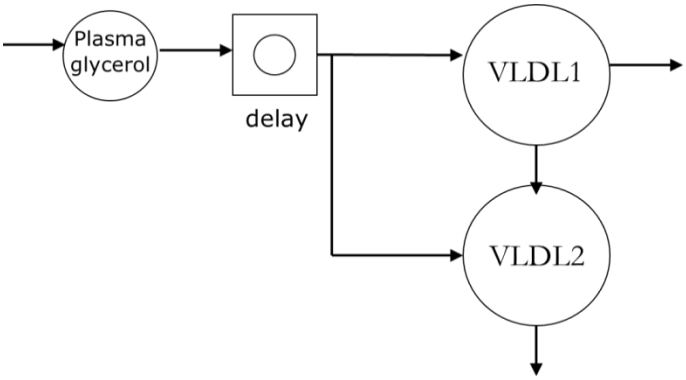

Figure 1. *Schematic description of the model used to describe TTRs of $VLDL_1$ and $VLDL_2$-TG.*

The model represents the kinetics of the tracer-to-tracee ratio (TTR) profiles which change as labelled glycerol is removed from plasma and incorporated into the TG fractions. The model assumes steady state of native (unlabelled) glycerol throughout the experimental period, i.e. a constant appearance, disappearance, and incorporation of native glycerol into the TG fractions. The model included a compartment for circulating $VLDL_1$-TG and a compartment for circulating $VLDL_2$-TG with an input into both compartments from the glycerol precursor pool in liver, a loss from each compartment and a transfer from the $VLDL_1$-TG compartment to the $VLDL_2$-TG compartment. Production rate (mg/kg/d) was calculated as the product of $VLDL_1$ and $VLDL_2$ FCR and the fraction TG pool sizes. The FCR for $VLDL_1$-TG transfer to $VLDL_2$-TG is termed $VLDL_1$-TG FCR transfer and the FCR for direct loss of $VLDL_1$-TG is termed $VLDL_1$-TG catabolism.

The direct input into $VLDL_2$-TG is termed $VLDL_2$-TG hepatic production rate and the transfer rate of TG from $VLDL_1$ to $VLDL_2$ is termed $VLDL_1$ to $VLDL_2$ transfer rate.

Kinetic modelling of apoB

$VLDL_1$ and $VLDL_2$, apoB FCR (pools/d) were determined using a model similar to that for $VLDL_1$ and VLDL2-TG, shown in Figure 1, using SAAM II software. αKIC was used as the intracellular precursor pool for protein synthesis and the model assumes a steady state concentration of unlabelled αKIC. The incorporation of αKIC into VLDL by the liver is subject to a delay accounting for the amount of time

required for synthesis and production rate of $VLDL_1$ and $VLDL_2$-apoB. Similar to the TG model, the delay compartment consisted of a five-compartment chain. Production rate (mg/kg/d) was calculated as the product of $VLDL_1$ and $VLDL_2$-apoB FCR and their respective apoB pool sizes.

In both models the parameters were estimated using weighted nonlinear regression analysis. The weights were reciprocal to the variance of the measurement error. The measurement error was assumed uncorrelated with zero mean; a constant standard deviation of 0.005% below TTR of 0.1% and a constant coefficient of variation of 5% above TTR of 0.1%.

References

1**. Hickson SS, Butlin M, Broad J, Avolio AP, Wilkinson IB, McEniery CM**. Validity and repeatability of the Vicorder apparatus: a comparison with the SphygmoCor device. *Hypertens Res*. 2009;32(12):1079-85.

2. **Thomas EL, Fitzpatrick JA, Malik SJ, Taylor-Robinson SD, Bell JD.** Whole body fat: content and distribution. *Prog Nucl Magn Reson Spectrosc*. 2013;73:56-80.

3. **Naressi A, Couturier C, Devos JM, et al**. Java-based graphical user interface for the MRUI quantitation package. *MAGMA.* 2001;12(2-3): 141-152.

4. **Christ ER, Cummings MH, Jackson N, et al.** Effects of growth hormone (GH) replacement therapy on low-density lipoprotein apolipoprotein B100 kinetics in adult patients with GH deficiency: a stable isotope study. *J Clin Endocrinol Metab.* 2004;89(4):1801-1807.

5. **Sarac I, Backhouse K, Shojaee-Moradie F, et al.** Gender differences in VLDL1 and VLDL2 triglyceride kinetics and fatty acid kinetics in obese postmenopausal women and obese men. *J Clin Endocrinol Metab.* 2012;97(7):2475-2481.

Supplement Table 1 Dietary intake

	Pre Ex n=12*	Post Ex n=12*	Within group p value	Pre Control n=10*	Post Control n=10*	Within group p value	Between group p value
Energy (MJ/d)	9.9±0.8	10.2±0.7	NS	8.7±0.5	8.2±0.5	NS	NS
Protein (g/d)	105±10	105±7	NS	89±8	83±7	NS	NS
Carbohydrate (g/d)	279±23	272±24	NS	208±6	203±11	NS	NS
Sugars (g)	102±13	111±16	NS	76±6	71±8	NS	NS
Fat (g/d)	87±9	96±9	NS	82±8	72±8	NS	NS
Saturated fat (g/d)	33±4	32±4	NS	30±3	25±3	NS	NS
Fibre (g/d)	29±6	37±13	NS	17±2	18±1	NS	NS
Sodium (g/d)	3.5±0.4	2.9±0.5	NS	2.9±0.3	2.7±0.2	NS	NS

*Three subjects in the exercise groups and two subjects in the control group failed to complete both diet dairies